

File ID 104704
Filename 3: Er-doped large band gap hosts

SOURCE (OR PART OF THE FOLLOWING SOURCE):

Type Dissertation
Title Time-Resolved Spectroscopy of Energy Transfers in Optoelectronic Media
Author I.Y. Izeddin Aguirre
Faculty Faculty of Science
Year 2008
Pages viii, 114

FULL BIBLIOGRAPHIC DETAILS:

<http://dare.uva.nl/record/270094>

Copyright

It is not permitted to download or to forward/distribute the text or part of it without the consent of the author(s) and/or copyright holder(s), other than for strictly personal, individual use.

3 Er-doped large band gap hosts

*They sentenced me to twenty years of boredom
For trying to change the system from within
I'm coming now, I'm coming to reward them*

...

Leonard Cohen, "First we take Manhattan"

3.1 Photoluminescence and excitation spectroscopy of Er³⁺ in GaN

The infrared photoluminescence at 1.5 μm due to the ${}^4\text{I}_{13/2} \rightarrow {}^4\text{I}_{15/2}$ transition of Er³⁺ ions has been investigated for GaN:Er³⁺ layers grown by MBE. Low temperature high resolution measurements performed under continuous illumination at the wavelength $\lambda_{exc} = 532 \text{ nm}$, quasi resonant to one of the intra 4f-shell transitions, revealed that the 1.5 μm band consists of up to eight individual spectral components. In excitation spectroscopy, a temperature dependent splitting of resonant bands was observed. Based on these experimental results, a possible multiplicity of optically active centers formed by Er doping in GaN layers is discussed.

3.1.1 Results

For over a decade, rare earth (RE) doped III-V semiconductors are widely investigated for their photonic properties and applications in optoelectronics [107, 108]. GaN as a host for RE ions is of interest due to its wide band gap, that guarantees luminescence at room temperature [109]. Er doping of GaN has been successfully used for fabrication of green light emitting devices [110].

Such a material is also interesting for luminescence at $1.5 \mu\text{m}$, coincident with the minimum absorption losses in optical fibers. The $1.5 \mu\text{m}$ emission from GaN:Er^{3+} is the focus of this section. The GaN:Er^{3+} samples used for these experiments were kindly provided by Dr. A.J. Steckl, from the University of Cincinnati; these were grown on a p-type (111) Si substrate, using the Solid Source Molecular Beam Epitaxy (SSMBE) method, after deposition of an AlN buffer layer. Details of preparation procedure can be found in Ref. [111]. The experiments described in this section were carried on a particular sample grown at an Er cell temperature of 860°C , Ga cell temperature of 935°C and substrate temperature of 650°C . The concentration of Er was $[\text{Er}] \approx 1 \text{ at.}\%$.

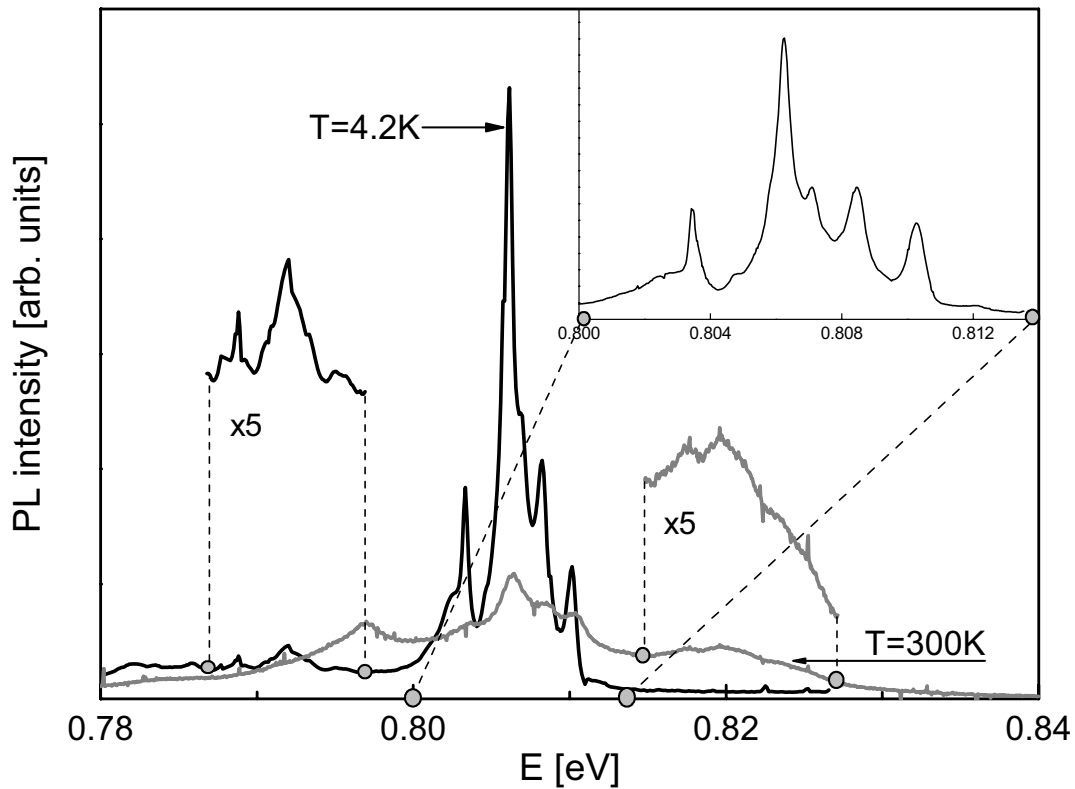


Figure 3.1: ${}^4I_{13/2} \rightarrow {}^4I_{15/2}$ emission spectrum from GaN:Er^{3+} under excitation to the ${}^2H_{11/2}$ multiplet ($\lambda_{exc} = 532 \text{ nm}$), recorded at 4.2 K (black line) and room temperature (grey line); phonon replica and anti-Stokes luminescence are shown five-fold amplified. Inset: high resolution spectrum for the main band at 4.2 K (range $0.800\text{--}0.814 \text{ eV}$).

Figure 3.1 shows the integrated intensity of the $1.5 \mu\text{m}$ PL band originating from the ${}^4I_{13/2} \rightarrow {}^4I_{15/2}$ Er^{3+} intra-4f shell transition. The sample was excited resonantly with a Nd:YVO_4 based laser operating in a continuous mode at $\lambda_{exc} = 532 \text{ nm}$, on-off modulated with a mechanical chopper. The sample was placed in a He gas flow cryostat and the measurements were taken at 4.2

K-to-room temperature range. PL signal was dispersed with a high resolution 1 m spectrometer and detected with a Ge detector. A photo multiplier tube was used to record decay kinetics of the PL signal.

The black line in Fig. 3.1 presents the PL spectrum of the sample in the 1.5 μm range taken at 4.2 K. A phonon replica of the band can be seen at energy lower by 14 meV. Such a separation does not coincide with the optical phonon in GaN, so a local phonon is probably involved. The grey line in the figure shows the PL spectrum at room temperature. A similar band is repeated at 14 meV above the main spectrum, representing anti-Stokes luminescence. The inset to the figure depicts a high resolution scan of the main PL band at 4.2 K: up to eight well resolved peaks can be distinguished.

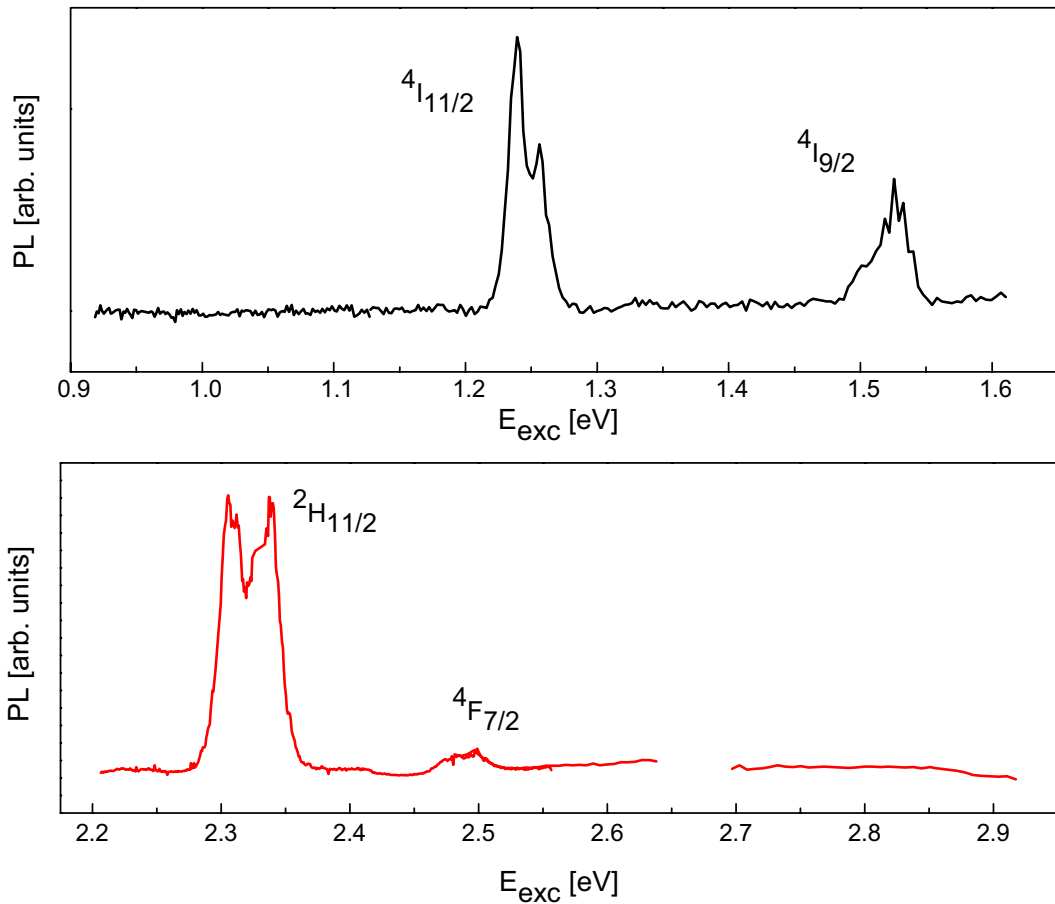


Figure 3.2: *PLE spectrum at 1537 nm (0.807 eV) taken at room temperature. Excitation is provided by a pulsed OPO. Individual bands are identified with the corresponding intra-4f transitions.*

Figure 3.2 shows the integrated room temperature PL intensity of the 1.5 μm band as a function of excitation energy (PLE). The tunable sub-band

excitation was provided by a Nd:YAG pumped optical parametric oscillator. The 350.4 nm line of an Ar⁺ ion laser was used for over-band gap excitation. As can be seen, in the regime of below band gap excitation only energies resonant with one of the 4f shell transitions lead to the 1.5 μm emission. The individual PLE bands can be identified with transitions from the ground state ($^4I_{15/2}$) to the $^4I_{11/2}$, $^4I_{9/2}$, $^2H_{11/2}$ and $^4F_{7/2}$ excited states, respectively. In addition, we note that three of the PLE bands split in two components; their separation differs per band.

3.1.2 Discussion

The observed splitting of the PLE bands (Fig. 3.2), together with the multiple structure reported in the high resolution spectrum (Fig. 3.1), can indicate existence of more than one type of Er-related optically active center in the studied sample. We investigated this possibility further by monitoring the 1.5 μm band under selective excitation tuned to individual components of the PLE bands. Identical spectra have been obtained with $E_{exc} = 1.23, 1.25, 1.48, 1.51, 2.31, 2.35$ and 2.50 eV. Also for over band gap excitation (3.54 eV) no difference has been seen in the structure of the 1.5 μm PL band. We also investigated the decay characteristics of individual components of the 1.5 μm band under selective excitation and found no differences as nearly identical decay times were measured independently of the excitation energy. Finally, the PLE spectra taken at a range of temperatures from 10 K to room temperature are depicted in Fig. 3.3. We observe that the relative intensity of the two components for each PLE band changes with temperature. While the higher energy component of the band enhances at lower temperatures, the lower energy component quenches and disappears.

Er ³⁺ level	E position (eV)	E splitting (meV)
$^4I_{15/2}$	0	12
$^4I_{11/2}$	1.25	3.8
$^4I_{9/2}$	1.5	11
$^2H_{11/2}$	2.3	23.6

Table 3.1: *Splitting of Er³⁺ states as deduced from the temperature dependence of the PLE bands.*

Taking into account the Er³⁺ levels splitting due to the crystal field, we will try to interpret the double structure of the PLE bands and its temperature dependence considering thermalization within the ground state. At low temperatures, only the lowest level at the ground energy state is populated. At a

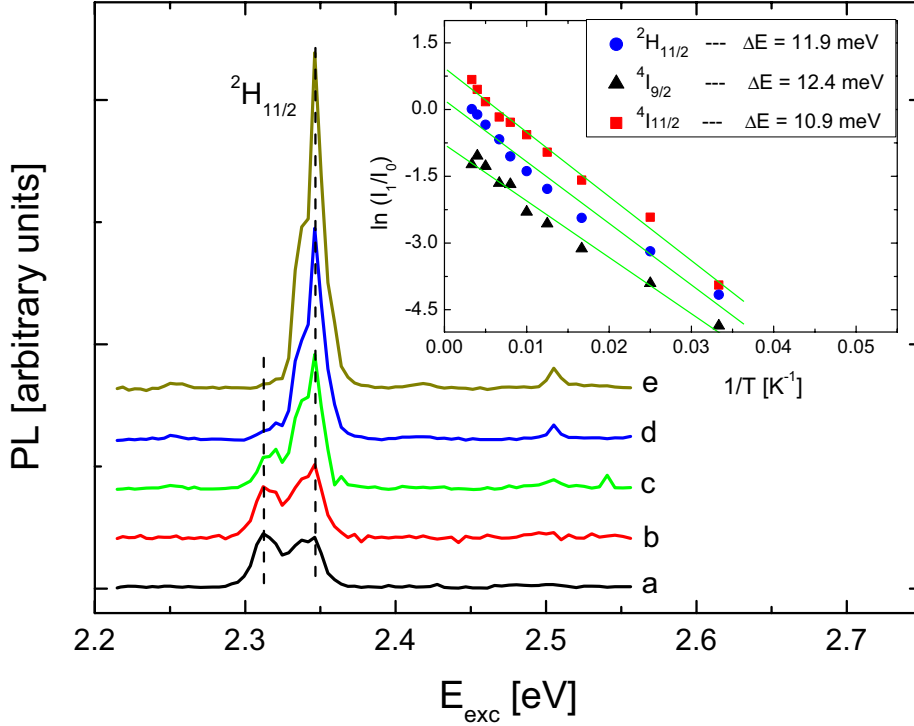


Figure 3.3: Temperature dependence of the ${}^2H_{11/2}$ excitation band, monitored with the spectrometer set at 1537 nm. $T = 300, 200, 100, 50$ and 10 K from (a) to (d), respectively. In the inset to the figure, Arrhenius plots of intensity ratio of 2 components of individual PLE bands are given.

higher temperature, Er^{3+} ions thermalize and populate upper levels leading to appearance of new components in the PLE band. Since not only the ground state, but also the excited states of Er^{3+} ions will be split, the energy distance between the components can be different for specific PLE bands and also not coincident with the ground state splitting.

In this simple model, for each excitation wavelength, the luminescence intensity is proportional to population of the ground state level. If we consider splitting of the ground state into 2 levels, the upper one being populated by thermalization from the lower one, the intensity ratio of the PLE band components I_1/I_0 will be given as:

$$I_1/I_0 \propto N_1/N_0 = A \exp(-\Delta E/k_B T), \quad (3.1)$$

where N_1 , N_0 , ΔE and k_B are populations in the upper and the lower ground state levels, the ground state splitting and the Boltzmann constant, respectively. In the inset of Fig. 3.3, the intensity ratio of the two components of the three investigated PLE bands is plotted versus the inverse of temperature. A

similar activation energy of $\Delta E \approx 12$ meV is obtained for all of them. Following the assumed model, this value corresponds to the energy separation within the ground state. Based on this, we can estimate the excited states splitting—see Table 3.1. We can conclude that the experimental data obtained thus far can be satisfactorily interpreted involving only one type of optically active Er^{3+} center in the investigated GaN layers.

3.2 On 2.7 μm emission from Er-doped large band gap hosts

The potential of Er-doped Cs_2NaYF_6 and GaN for mid-infrared emission at $\lambda \approx 2.7 \mu\text{m}$ is investigated using time-resolved optical spectroscopy. This emission results from electronic transitions between the second (${}^4\text{I}_{11/2}$) and first (${}^4\text{I}_{13/2}$) excited states of the Er^{3+} ion. By recording the photoluminescence transients for the ${}^4\text{I}_{11/2} \rightarrow {}^4\text{I}_{15/2}$ and ${}^4\text{I}_{13/2} \rightarrow {}^4\text{I}_{15/2}$ transitions after pulsed excitation, we determine the lifetime of the ${}^4\text{I}_{11/2}$ level and demonstrate that the ${}^4\text{I}_{13/2}$ state is populated from this level. Our results indicate that both hosts should enable 2.7 μm emission, whose intensity is temperature-stable but subject to concentration quenching.

3.2.1 Introduction

Mid-infrared laser radiation in the 2 - 3 μm range has applications in the fields of remote sensing, trace gas monitoring, and laser surgery [112]. Currently, optically (flashlamp or diode) pumped rare-earth RE-doped insulating inorganic crystals or glasses are used as laser sources in this range [113]. Especially for laser surgery applications, research towards tunable and more compact, electrically pumped sources is still ongoing. In the past few years, $\text{ZnSe}:\text{Cr}^{2+}$ has emerged as widely tunable laser medium, covering the complete 2 - 3 μm range, but electrical pumping of such crystals is yet to be demonstrated [112, 114]. The design of more compact MIR lasers has focused towards diode-pumped fiber lasers [115]. However, electrically pumped media, preferably compatible with Si technology, would result in possible development of even cheaper and more compact sources. Visible electroluminescence from RE doped hexagonal GaN, epitaxially grown on Si substrates, has already been demonstrated several years ago [110]. Recently, a CMOS-compatible spin coating technique for GaN powders on Si has been developed and green luminescence has been obtained from Er-doped powders [116]. As the intra-4f transition between the second (${}^4\text{I}_{11/2}$) and first (${}^4\text{I}_{13/2}$) excited states of the Er^{3+} ion is in the range of interest (2.7 - 3.0 μm , depending on the host), it is interesting to explore the potential of Er-doped GaN as active MIR lasing medium.

In the present work, we address temporal aspects of the ${}^4\text{I}_{11/2} \rightarrow {}^4\text{I}_{13/2}$ transition of Er^{3+} in GaN, as well as possible luminescence quenching mechanisms. To this end, the kinetics of photoluminescence for the ${}^4\text{I}_{11/2} \rightarrow {}^4\text{I}_{15/2}$ transition at $\lambda \approx 1.0 \mu\text{m}$ and the ${}^4\text{I}_{13/2} \rightarrow {}^4\text{I}_{15/2}$ transition at $\lambda \approx 1.5 \mu\text{m}$ are studied. We hereby take advantage of the highly sensitive and fast detectors, developed for this wavelength range. Meanwhile, special precautions, to be taken when directly detecting radiation with $\lambda > 2.5 \mu\text{m}$ in order to prevent

absorption by air (water) and commonly used silica lenses, are avoided. In a similar way, we have also studied Er^{3+} -doped Cs_2NaYF_6 . In this crystal Er^{3+} can only be incorporated on Y^{3+} positions, which have O_h point group symmetry and are widely spaced (nearest neighbor distance 0.64 nm [117]). As these crystals accept Er concentrations up to 100% (all Y^{3+} ions substituted), they present a good model system for investigating the influence of Er-concentration on the 2.7 μm emission.

3.2.2 Experimental details

The $\text{Cs}_2\text{NaY}_{1-x}\text{Er}_x\text{F}_6$ crystals ($x = 0.001, 0.01, 0.1, \text{ and } 1$) were hydrothermally grown, using Er_2O_3 as dopant [118]. The hexagonal $\text{GaN}:\text{Er}^{3+}$ samples were epitaxially grown on a p-type (111) Si substrate, after deposition of an AlN buffer layer, using the solid source molecular beam epitaxy method [111]. The Er-concentration in these samples is estimated at 1 at.%.

Time-resolved PL measurements were performed using a Nd:YAG-pumped optical parametric oscillator as tunable pulsed laser excitation source, generating 5 ns pulses, with a maximum energy of 1 mJ, at a repetition rate of 10 Hz in the $\lambda = 410 - 2200$ nm range. For measurements at low temperature, the GaN samples, which exhibit good thermal conductivity, were placed in a closed-cycle cryostat, with a minimum operation temperature of ~ 20 K, whereas for the poorly conducting Cs_2NaYF_6 crystals a He flow cryostat was used. The luminescence light was dispersed with a 1 m monochromator and detected with a liquid N_2 -cooled InGaAs photomultiplier (300 - 1700 nm). For the slow kinetics in Cs_2NaYF_6 the excitation repetition rate was lowered by blocking laser pulses with a shutter. The detector was operated in photon counting mode for detecting the much faster kinetics of Er^{3+} in GaN.

3.2.3 Results and discussion

In Fig. 3.4 the TR PL for the ${}^4\text{I}_{11/2} \rightarrow {}^4\text{I}_{15/2}$ and ${}^4\text{I}_{13/2} \rightarrow {}^4\text{I}_{15/2}$ transitions in a 1% Er^{3+} -doped $\text{Cs}_2\text{NaY}_{(1-x)}\text{F}_6$ crystal ($x = 0.01$), measured at 4.2 K, is shown. In view of the large average dopant ion spacing at this concentration, only limited effects of Er-Er interactions and energy migration between Er^{3+} ions are expected. The PL transients are analyzed assuming first order decay kinetics in an atomic three levels system (see excitation schemes in Fig. 3.4), leading to

$$I_{PL}(t) = A(e^{-t/\tau_d} - e^{-t/\tau_r}), \quad (3.2)$$

where τ_r and τ_d represent the rise and decay times of the signal, respectively, which correspond to the population time and lifetime of the upper level involved in the detected luminescence transition. Traces (a) and (b) are recorded

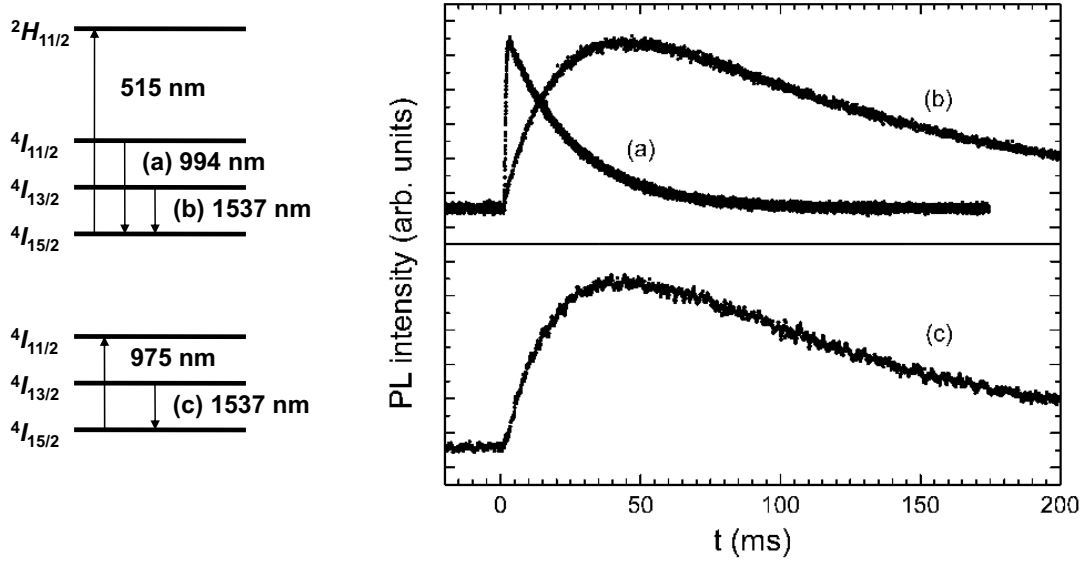


Figure 3.4: Time resolved PL of the transitions from the second and first excited states of Er^{3+} in $\text{Cs}_2\text{NaY}_{1-x}\text{Er}_x\text{F}_6$ ($x = 0.01$) at 4.2 K. PL excitation schemes are shown at the left.

after exciting the Er^{3+} ions to the ${}^2\text{H}_{11/2}$ level, which presents the highest excitation efficiency for 1.54 μm emission. The TR PL from the second excited state is perfectly reproduced assuming a rise time of 0.5 ms and a decay time of 21 ms. Although in principle several relaxation paths from the ${}^2\text{H}_{11/2}$ to the ${}^4\text{I}_{13/2}$ are possible, the kinetics of luminescence from the first excited state show a single rise time of 21 ms and a decay time of 100 ms. These results indicate that the lifetimes of the second and first excited states of Er^{3+} in Cs_2NaYF_6 are 21 and 100 ms, respectively, and that the ${}^4\text{I}_{13/2}$ state is (nearly) exclusively populated from the ${}^4\text{I}_{11/2}$ level. In order to check the lifetime assignments, the TR PL from the ${}^4\text{I}_{13/2}$ level has also been recorded after excitation to the second excited state (trace (c)). Essentially the same kinetics as for excitation to the ${}^2\text{H}_{11/2}$ level are observed. In this way we rule out the possibility that the measured decay time of the ${}^4\text{I}_{11/2} \rightarrow {}^4\text{I}_{15/2}$ transition would correspond to the lifetime of some intermediate long living state in the decay path from the ${}^2\text{H}_{11/2}$ level. Thus, it is demonstrated that transitions between the second and first excited states of Er^{3+} take place in these crystals and the long lifetimes of the levels involved indicate that they occur to large extent by radiative decay.

In order to examine possible quenching mechanisms for this luminescence, the lifetime of the ${}^4\text{I}_{11/2}$ level has also been measured at room temperature and for other Er^{3+} concentrations. The results, summarized in Table 3.2,

x	4.2 K	300 K
0.001	21 ₃	9 ₂
0.01	21 ₃	12 ₂
0.1	1.4 ₂	1.1 ₂
1	1.1 ₂	0.7 ₂

Table 3.2: Lifetime (in ms) of the Er^{3+} $^4I_{11/2}$ level in $Cs_2NaY_{1-x}Er_xF_6$ at 4.2 K and room temperature. The error in the last digit is indicated as a subscript.

show that temperature only has a minor effect on the $2.7 \mu\text{m}$ luminescence. In contrast, at high Er-concentrations an important quenching of the $^4I_{11/2}$ lifetime is observed, most probably as a result of interactions (cross-relaxation, upconversion) between Er^{3+} ions.

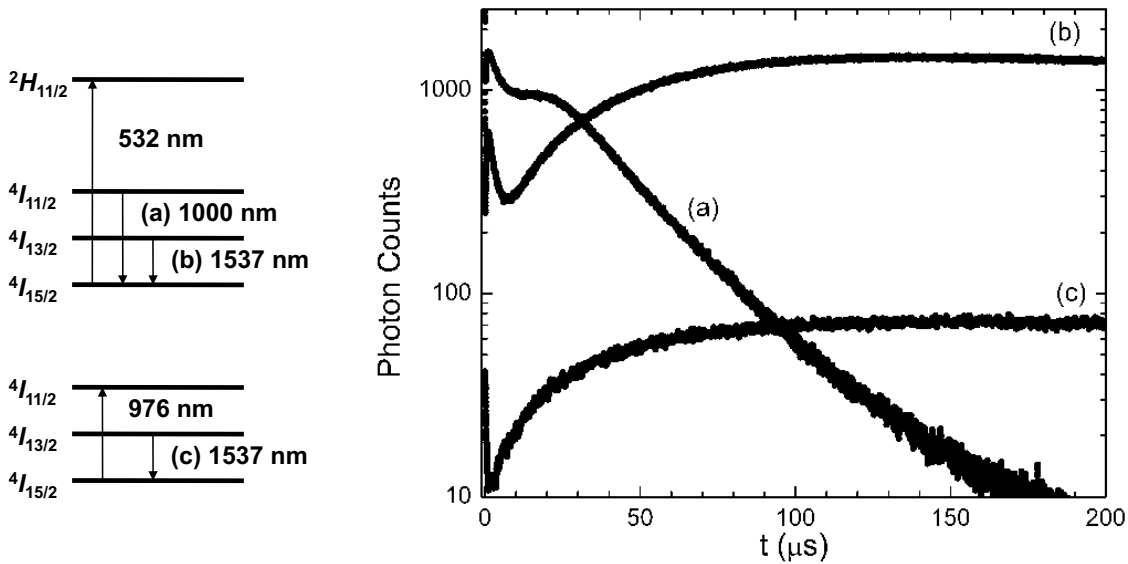


Figure 3.5: Time resolved PL of the transitions from the second and first excited states of Er^{3+} in GaN (1 at.% doping concentration) at 20 K. PL excitation schemes are shown at the left.

Figure 3.5 presents PL transients for a 1% Er^{3+} -doped GaN sample at 20 K. These signals have a more complicated time-dependence than those for the insulating material. A fast component, observed in the traces after excitation to the $^2H_{11/2}$ level ((a) and (b)) with a decay time of $\sim 3 \mu\text{s}$, is most probably related to visible green emission ($^4S_{3/2} \rightarrow ^4I_{15/2}$). The slow components hereafter do not exhibit single first order decay kinetics, as described by Eq. 3.2. This is most probably a result of the formation of multiple Er^{3+} centers

in these samples, as earlier reported for similarly grown structures [119]. The TR PL corresponding to the ${}^4\text{I}_{11/2} \rightarrow {}^4\text{I}_{15/2}$ transition (trace (a)) has a rise time of 7 - 10 μs and a decay time of 20 - 40 μs . The sum of these time constants roughly corresponds to the rise time of the ${}^4\text{I}_{13/2} \rightarrow {}^4\text{I}_{15/2}$ transition (30 - 50 μs , trace(b)). After direct excitation to the ${}^4\text{I}_{11/2}$ level, the latter transition has a rise time in the 30 - 40 μs range (trace(c)). These results thus show that the lifetime of the second excited state of Er^{3+} in this sample is 20 - 40 μs and the cumulative lifetime of the intermediate levels (${}^2\text{H}_{11/2} \rightarrow {}^4\text{I}_{11/2}$) amounts to 7 - 10 μs . The lifetime of the first excited state is found in the 1 - 1.5 ms range. In addition, it is demonstrated that the population of the ${}^4\text{I}_{13/2}$ level is dominated by transitions from the second excited state. At room temperature, the lifetime of the ${}^4\text{I}_{11/2}$ level is found to be $\sim 18 \mu\text{s}$. Again, no dramatic temperature quenching is observed for this transition.

As 2.7 μm emission from GaN:Er^{3+} is envisaged, it still has to be demonstrated that radiative transitions between the ${}^4\text{I}_{11/2}$ and the ${}^4\text{I}_{13/2}$ levels take place. Comparing the results for GaN with those for Cs_2NaYF_6 at low Er concentration, we find that the rise time of the ${}^4\text{I}_{11/2} \rightarrow {}^4\text{I}_{15/2}$ transition and the lifetime of the ${}^4\text{I}_{13/2}$ level are ~ 70 times shorter. The lifetime of the second excited state of Er^{3+} , however, appears to be shortened by an additional factor of ~ 8 , pointing to some non-radiative decay mechanism. One might consider multi-phonon relaxation between the ${}^4\text{I}_{11/2}$ and the ${}^4\text{I}_{13/2}$ level, which would imply that practically no radiative transitions between these levels occur. As only 5 longitudinal optical (LO) lattice phonons ($\hbar\Omega \sim 90 \text{ meV}$ [120]) are required to bridge the gap between the second and first excited state, multi-phonon relaxation may indeed be important [121]. This would, however, further imply that the lifetimes of the ${}^4\text{S}_{3/2}$ and ${}^4\text{F}_{9/2}$ levels experience an even stronger non-radiative quenching, as for these levels multi-phonon relaxation to the next state only requires 4 LO phonons. The rise time observed for the ${}^4\text{I}_{11/2} \rightarrow {}^4\text{I}_{15/2}$ transition and the occurrence of visible luminescence from these higher excited states (see *e.g.* [119]) do not support such a quenching mechanism. In fact, observations of phonon replicas in the PL of GaN:Er^{3+} rather suggest coupling to the transverse optical (TO) phonon mode ($\hbar\Omega \sim 68 \text{ meV}$) with a very small coupling strength ($S = 0.02$) [119] or to a local vibrational mode (14 meV) [122]—see previous section. In either case, multi-phonon relaxation is not expected to dominate the ${}^4\text{I}_{11/2} \rightarrow {}^4\text{I}_{13/2}$ transition. On the other hand, the doping level of the GaN sample is comparable to that of the $\text{Cs}_2\text{NaY}_{0.9}\text{Er}_{0.1}\text{F}_6$ crystal, for which an important concentration quenching of the ${}^4\text{I}_{11/2}$ lifetime is seen. We therefore believe that the 2.7 μm emission from the GaN sample is also strongly quenched by interactions between Er^{3+} ions, which are possibly related with the appear-

ance of visible (green, red) luminescence as well. Further experiments on GaN crystals with lower Er-concentrations are being undertaken in order to verify these hypotheses.

3.2.4 Conclusions

From time-resolved photoluminescence measurements in the near IR for a $\text{Cs}_2\text{NaY}_{1-x}\text{Er}_x\text{F}_6$ concentration series and for a 1 at.% Er^{3+} -doped GaN sample, we have determined the lifetime of the second excited state of the Er^{3+} ion and shown that the first excited state is predominantly populated through $^4\text{I}_{11/2} \rightarrow ^4\text{I}_{13/2}$ transitions. It is argued that the latter transitions are not governed by multi-phonon relaxation. Hence, it is demonstrated that these materials should exhibit $2.7 \mu\text{m}$ emission, which is almost independent of temperature, but most likely shows an important concentration quenching. Realization of electrically driven MIR emission from Er-doped GaN, compatible with Si technology, thus seems feasible.